

Article

Astragaloside IV Suppresses Hepatic Proliferation in Regenerating Rat Liver after 70% Partial Hepatectomy via Down-Regulation of Cell Cycle Pathway and DNA Replication

Gyeong-Seok Lee ¹, Hee-Yeon Jeong ¹, Hyeon-Gung Yang ², Young-Ran Seo ¹, Eui-Gil Jung ³, Yong-Seok Lee ¹ , Kung-Woo Nam ¹ and Wan-Jong Kim ^{1,*} 

¹ Department of Life Science and Biotechnology, College of Natural Sciences, Soonchunhyang University, Asan 31538, Chungcheongnam-do, Korea; ssm4914@naver.com (G.-S.L.); youn6640@naver.com (H.-Y.J.); 94seoyoung@gmail.com (Y.-R.S.); yslee@sch.ac.kr (Y.-S.L.); kwnam1@sch.ac.kr (K.-W.N.)

² Soonchunhyang Institute of Medi-bio Science (SIMS), Soonchunhyang University, Cheonan 31151, Chungcheongnam-do, Korea; yhg930205@naver.com

³ Seoul Center, Korea Basic Science Institute, Seoul 02855, Korea; euigiljung@gmail.com

* Correspondence: wjkim56@sch.ac.kr; Tel.: +82-41-530-1251

Abstract: Astragaloside IV (AS-IV) is one of the major bio-active ingredients of huang qi which is the dried root of *Astragalus membranaceus* (a traditional Chinese medicinal plant). The pharmacological effects of AS-IV, including anti-oxidative, anti-cancer, and anti-diabetic effects have been actively studied, however, the effects of AS-IV on liver regeneration have not yet been fully described. Thus, the aim of this study was to explore the effects of AS-IV on regenerating liver after 70% partial hepatectomy (PHx) in rats. Differentially expressed mRNAs, proliferative marker and growth factors were analyzed. AS-IV (10 mg/kg) was administrated orally 2 h before surgery. We found 20 core genes showed effects of AS-IV, many of which were involved with functions related to DNA replication during cell division. AS-IV down-regulates MAPK signaling, PI3/Akt signaling, and cell cycle pathway. Hepatocyte growth factor (HGF) and cyclin D1 expression were also decreased by AS-IV administration. Transforming growth factor β 1 (TGF β 1, growth regulation signal) was slightly increased. In short, AS-IV down-regulated proliferative signals and genes related to DNA replication. In conclusion, AS-IV showed anti-proliferative activity in regenerating liver tissue after 70% PHx.

Keywords: astragaloside IV; *Astragalus membranaceus*; huang qi; Astragali Radix; liver; liver regeneration; 70% partial hepatectomy; proliferation; rat



Citation: Lee, G.-S.; Jeong, H.-Y.; Yang, H.-G.; Seo, Y.-R.; Jung, E.-G.; Lee, Y.-S.; Nam, K.-W.; Kim, W.-J. Astragaloside IV Suppresses Hepatic Proliferation in Regenerating Rat Liver after 70% Partial Hepatectomy via Down-Regulation of Cell Cycle Pathway and DNA Replication. *Molecules* **2021**, *26*, 2895. <https://doi.org/10.3390/molecules26102895>

Academic Editors: Raffaele Pezzani and Sara Vitalini

Received: 19 April 2021

Accepted: 11 May 2021

Published: 13 May 2021

Publisher's Note: MDPI stays neutral with regard to jurisdictional claims in published maps and institutional affiliations.



Copyright: © 2021 by the authors. Licensee MDPI, Basel, Switzerland. This article is an open access article distributed under the terms and conditions of the Creative Commons Attribution (CC BY) license (<https://creativecommons.org/licenses/by/4.0/>).

1. Introduction

For a long time, medicinal plants have played a key role in pharmacological research studies and drug development. *Astragalus membranaceus* is medicinal plant that has been used in traditional Chinese medicine throughout history; it is also called Astragali Radix. Huang qi (黄芪, in Chinese) is the name for the dried root of *Astragalus membranaceus* and it is mainly produced in China, Mongolia, and Korea [1]. The main components of huang qi are saponins, polysaccharides and flavonoids [2–4]. It has been used in traditional Chinese medicine for over 2000 years to treat various diseases including anemia, cardiovascular disorder, weakness, fatigue and fever [4,5]. In recent years, it has been reported that huang qi has anti-oxidative, anti-aging, anti-inflammatory, anti-diabetic, and anti-cancer properties [1–4].

Astragaloside IV (AS-IV) is a representative bio-active ingredient of huang qi [4,6]. AS-IV is classified as a tetra cyclic triterpenoid, otherwise known as a protostane which means prototype of steroid (Figure 1) [7]. AS-IV has a similar carbon-tetra-cyclic structure to steroids which have a bio-activities as cholesterol. Recently, it was reported that long-term dietary cholesterol overload negatively affects liver regeneration after PHx. Cholesterol overload reduced hepatic DNA synthesis [8]. While, other steroid, estradiol accelerates

liver regeneration [9]. Thus, it was expected that the AS-IV directly has an effects on liver regeneration after PHx. Many reports have shown that AS-IV has anti-oxidative properties and protective effects against hypoxic injury and ischemia-reperfusion injury [10–15]. The anti-cancer activities of AS-IV via inhibition of migration and invasion of cancer cells have also been demonstrated [16,17]. Moreover, AS-IV improves diabetic nephropathy, retinopathy, gastropathy, and wound healing [18–21] Hepato-protective effects against hepatic fibrosis, oxidative stress, and hepatitis B virus were also reported [10,22–25].

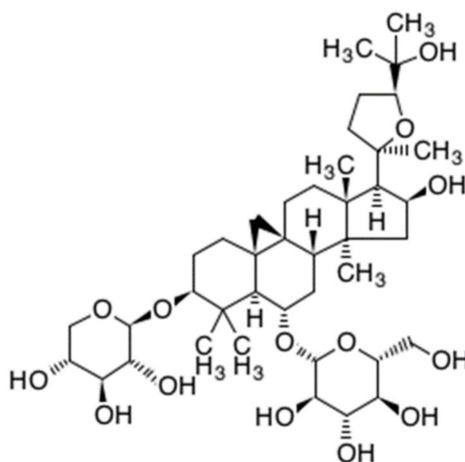


Figure 1. Chemical structure of astragaloside IV. ($C_{41}H_{68}O_{14}$, molecular weight: 794.97 g/mol).

The liver has ability to recover lost functional capacity after chemical or physical injury. After injury, the liver quickly regenerates to meet metabolic demand via the proliferation of hepatic cells. Liver regeneration involves a complex network of growth factors, signaling pathways, and transcriptional factors [26]. Uniquely, liver regeneration occurs without functional loss and through repopulation of mature cells rather than progenitor or stem cells [27].

The 70% partial hepatectomy (PHx) model is a commonly used model to investigate new aspects of liver regeneration [28]. It was first described by Higgins and Anderson in 1931. PHx is a surgical procedure to resect the median and left lateral lobes of the liver, which constitute about 70% of the liver mass [29–31]. Liver regeneration is especially rapid in small rodents; full-size restorations have been reported within 7 days in most rodents [27,32]. After PHx, remnant liver tissues undergo three phases. First is priming phase, which is characterized by the stimulation of hepatic mitogen. Hypoxic conditions after PHx and hemo-dynamic factors such as blood pressure are thought to be major stimulators of liver regeneration [33–36]. The liver is not alone in promoting its own regeneration, and cooperative signals for priming also come from the pancreas, spleen, duodenum, and adrenal glands [37,38]. Second is proliferating phase; DNA replication in hepatocytes started. The last step is growth termination. Transforming growth factor $\beta 1$ (TGF $\beta 1$) is secreted by non-parenchymal cells including hepatic stellate cells, Kupffer cells, and platelets. TGF $\beta 1$ plays an important role in ending regeneration through suppression of hepatic proliferation [33,39,40].

The pharmacological effects of AS-IV have been actively studied in recent years and hepato-protective effects of AS-IV have been extensively reported. However, the effects of AS-IV on liver regeneration are not yet fully elucidated. In this study, the effects of AS-IV were investigated in a 70% PHx rat model through measurement of gene expression, the expression of hepatocyte growth factor (HGF, primary hepatic mitogen), and the expression of hepatic proliferation marker protein.

2. Results

2.1. mRNA Sequencing Analysis

To determine the effects of AS-IV on the gene expression of regenerating liver tissues after PHx, changes of gene expression were measured 12 h after PHx by mRNA sequencing analysis. The count of differentially expressed genes (DEGs) was 17,048; DEGs exhibiting changes more than 2-fold were considered significant. DEGs exhibiting changes more than 2-fold and 5-fold were 975 and 103 genes, respectively (Figure 2a,b). In the results of the two-fold DEGs, 370 DEGs were up-regulated and 605 DEGs were down-regulated by AS-IV (Figure 2c). Results from the 5-fold DEGs showed that 31 DEGs were up-regulated and 72 DEGs were down-regulated by AS-IV (Figure 2d).

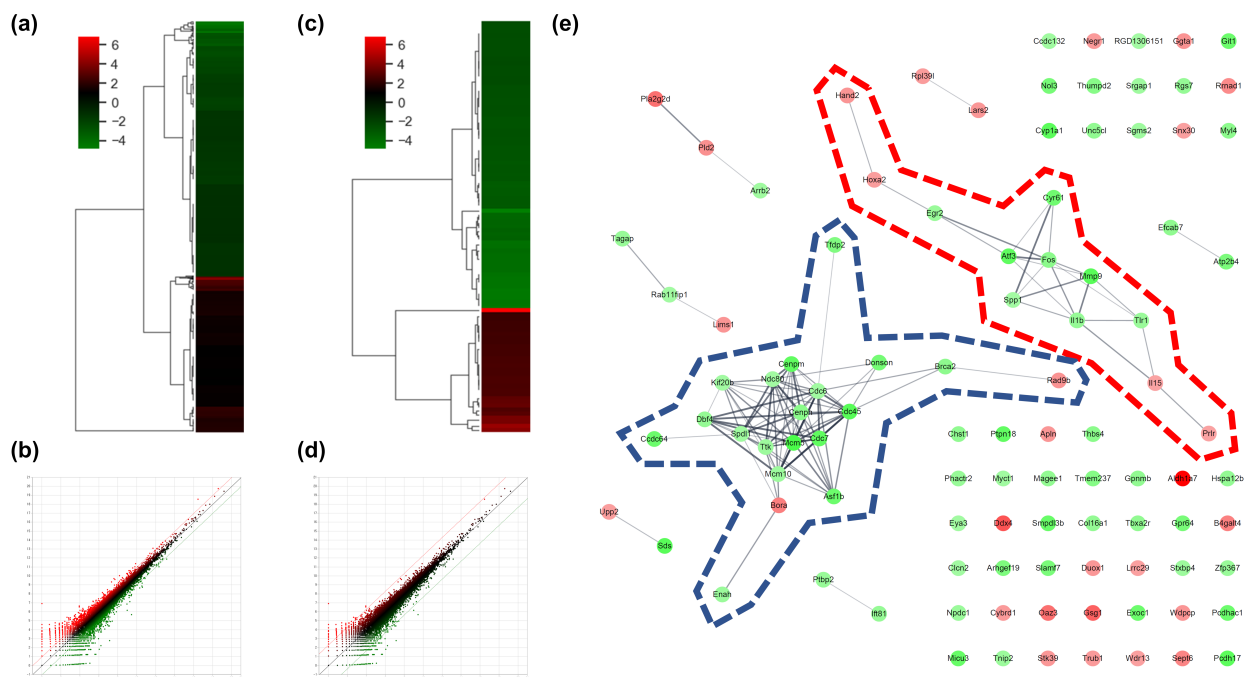


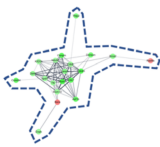

Figure 2. DEGs and gene network. (a) heatmap with hierarchical clustering of 2-fold changed DEGs, (b) expression pattern for 2-fold changed DEGs, (c) heatmap with hierarchical clustering of 5-fold changed DEGs, (d) expression pattern for 5-fold changed DEGs, (e) Gene network of 5-fold changed DEGs. 20 DEGs (in blue dotted line) and 12 DEGs (in red dotted line) were clustered. Markedly, DEGs within the blue dotted line showed strong relation. 14 other DEGs (not marked) were linked with only one or two genes. The green color in the figure indicates decreased expression; the red color in the figure indicates increased expression.

2.1.1. Key Gene Screening and Functional Annotation

To determine the pharmacological effects of AS-IV, we listed key genes from the result and investigated their function through corresponding protein of genes. We listed highly changed DEGs (more than 5-fold) and generated gene networks for the DEGs using a multiple protein search tool within the STRING database; two big cluster networks of DEGs were generated (Figure 2e). One network, which is marked by a blue dotted line in Figure 2e, consisted of 20 DEGs including *Mcm5*, *Cdc45*, *Cdc7*, *Cenpm*, *Asf1b*, *Donson*, *Tfdp2*, *Ccdc64*, *Cenpn*, *Brca2*, *Dbf4*, *Enahm*, *Mcm10*, *Ttk*, *Spdl1*, *Cdc6*, *Ndc80*, *Kif20b*, *Rad9b* and *Bora*. Another big network, marked by the red dotted line of Figure 2e, consisted of 12 genes including *Mmp9*, *Atf3*, *Cyr61*, *Fos*, *Il1b*, *Tlr1*, *Egr2*, *Spp1*, *Il15*, *Prlr*, *Hoxa2*, and *Hand2*. Functional annotation of DEGs in cluster network was conducted using the database for annotation, visualization and integrated discovery (DAVID) bioinformatic tool in three GO (gene ontology) categories including biological process, cellular component, molecular function (Table 1). The 20 DEGs in blue dotted line of Figure 2e were matched with

DNA replication initiation, cell division, double-strand break repair via break-induced replication, and DNA duplex unwinding, all of which fall within the biological process category. In the cellular component category, nucleoplasm was matched. In the molecular function category, DNA replication origin binding and chromatin binding were matched. Results from the functional annotation of the DEGs in this cluster (blue dotted line) showed that these genes were related to the DNA replication process of cell division. DEGs in the other clustered network within the red dotted line of Figure 2e were matched with positive regulation of angiogenesis, positive regulation of protein phosphorylation, and positive regulation of apoptotic process. They were matched only the biological process category (Table 1). From the changes in gene expression, strong interaction and function, we considered DEGs within the blue dotted line to be the key DEGs showing the effects of AS-IV.

Table 1. Functional annotation of clustered DEGs by DAVID in Figure 2e.

Gene network		
Clustered genes	<i>Mcm5, Cdc45, Cdc7, Cenpm, Asf1b, Donson, Tfdp2, Ccdc64, Cenpn, Brca2, Dbf4, Enahm, Mcm10, Ttk, Spdl1, Cdc6, Ndc80, Kif20b, Rad9b, Bora</i>	<i>Mmp9, Atf3, Cyr61, Fos, Il1b, Tlr1, Egr2, Spp1, Il15, Prlr, Hoxa2, Hand2</i>
GO category	<ul style="list-style-type: none"> - DNA replication initiation - Cell division - Double-strand break repair via break-induced replication - DNA duplex unwinding 	<ul style="list-style-type: none"> - Positive regulation of angiogenesis - Positive regulation of protein phosphorylation - Positive regulation of apoptotic process
Cellular component	- Nucleoplasm	(not matched)
Molecular function	<ul style="list-style-type: none"> - DNA replication origin binding - Chromatin binding 	(not matched)

2.1.2. Pathway Mapping of DEGs

DEGs exhibiting 2-fold changes were further analyzed using the KEGG pathway database to evaluate the effect of AS-IV on signaling in regenerating liver tissues. Remarkably, DEGs were highly matched with three pathways including MAPK signaling, PI3K-Akt signaling, and cell cycle pathways (Table 2). The DEGs in these three pathways showed similar down-regulated patterns; overall, most matched DEGs were down-regulated (Figure 3).

Table 2. Results of pathway mapping for 2-fold changed DEGs by AS-IV.

KEGG Pathway	Matched	Count of Genes	
		Up-Regulated	Down-Regulated
MAPK signaling pathway	24	5	19
PI3K-Akt signaling pathway	22	5	17
Cell cycle pathway	22	1	21

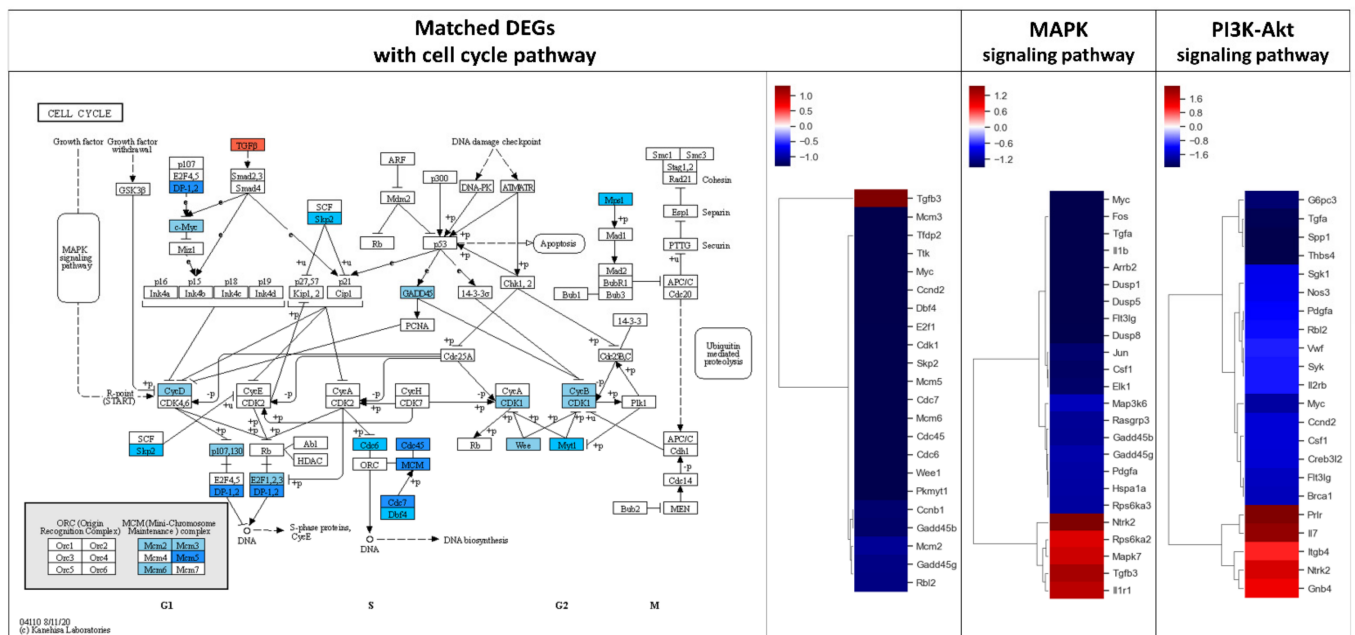


Figure 3. Results of KEGG pathway mapping. 2-fold changed DEGs were analyzed using the KEGG pathway database. 24, 22, and 22 DEGs were included in cell cycle, MAPK signaling, and PI3K-Akt signaling pathways, respectively. AS-IV showed down-regulatory effects on these pathways. Only a few DEGs were up-regulated in these three pathways. MAPK signaling and PI3K-Akt signaling pathways were upstream of the cell cycle pathway. The red and blue color in the figure indicate up-regulation and down-regulation of genes, respectively. Intensity of color is proportional to fold change.

2.2. Hepatic Proliferation of Regenerating Liver Tissue

Hepatic proliferation of regenerating liver tissue after AS-IV administration was evaluated via immunohistochemical staining and Western blot analysis for hepatocyte growth factor (HGF) (a mitogen for hepatocytes), cyclin D1 (a marker protein for proliferation), and transforming growth factor β 1 (TGF β 1) (a terminator for proliferation).

As HGF is a major stimulator of proliferation of hepatocyte during liver regeneration, the expression of HGF was evaluated to determine the hepato-proliferative signal after 70% PHx. Thus, the ratio of HGF positive cells increased immediately after 70% PHx and peaked 12 h after PHx. The ratio of immuno-positive cells in the AS-IV group showed a decrease when compared to controls (Figure 4). Remarkably, immediately after PHx, HGF expression decreased in half of the control group. Cyclin D1 was evaluated to determine the level of proliferation of hepatocyte after proliferative signal. It showed different expression. Cyclin D1 increased since 12 h after PHx with progression for cell cycle. In the AS-IV group, cyclin D1 expression was markedly decreased at 12 and 24 h after PHx (Figure 5). Results of Western blot analysis for cyclin D1 showed a decrease similar to that of the immunohistochemical results in Figure 5 (Figure 6). Cyclin D1 expression was dramatically decreased by AS-IV 24 h after PHx. TGF β 1 was also determined by Western blot analysis to be a signal of growth regulation (Figure 6). The expression of TGF β 1 showed no difference 12 h after PHx, however, it was slightly increased with AS-IV treatment 24 h after PHx.

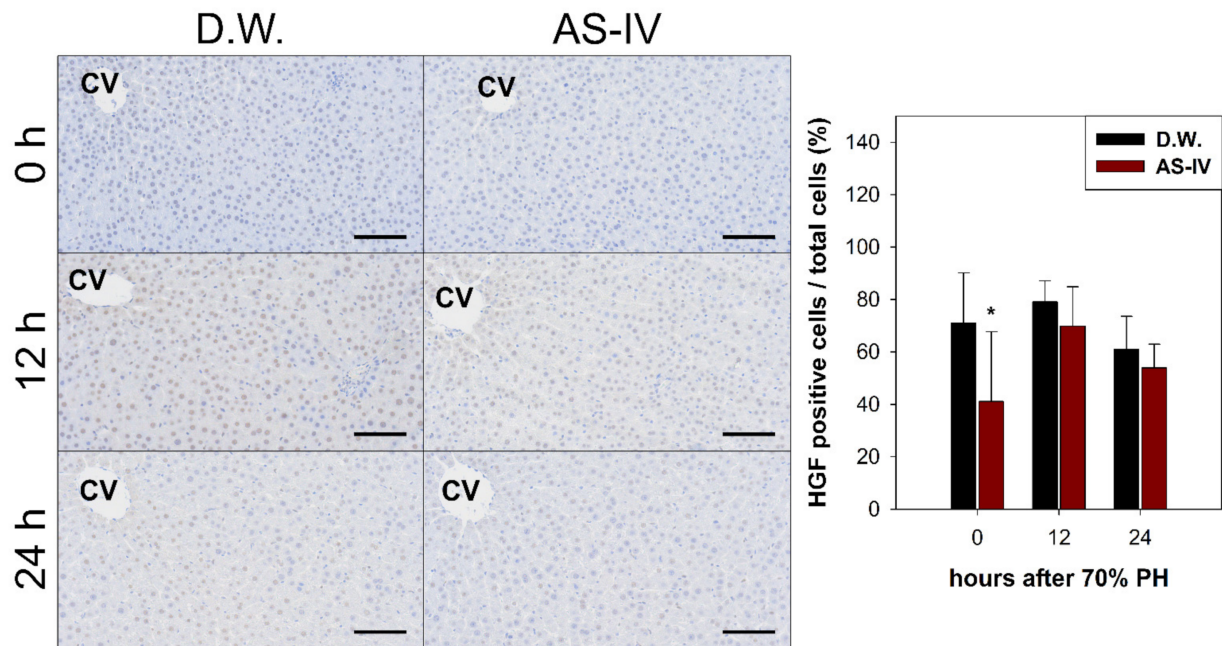


Figure 4. Immunostaining for HGF. HGF-immuno-positive reactions were a brown color after immunostaining. HGF peaked at 12 h after PHx. The AS-IV group showed a low expression of HGF. Hematoxylin was used as a counter stain. (Scale bar indicates 100 μ m, CV: central vein, $n = 3$, mean \pm standard deviation, *: $p < 0.05$).

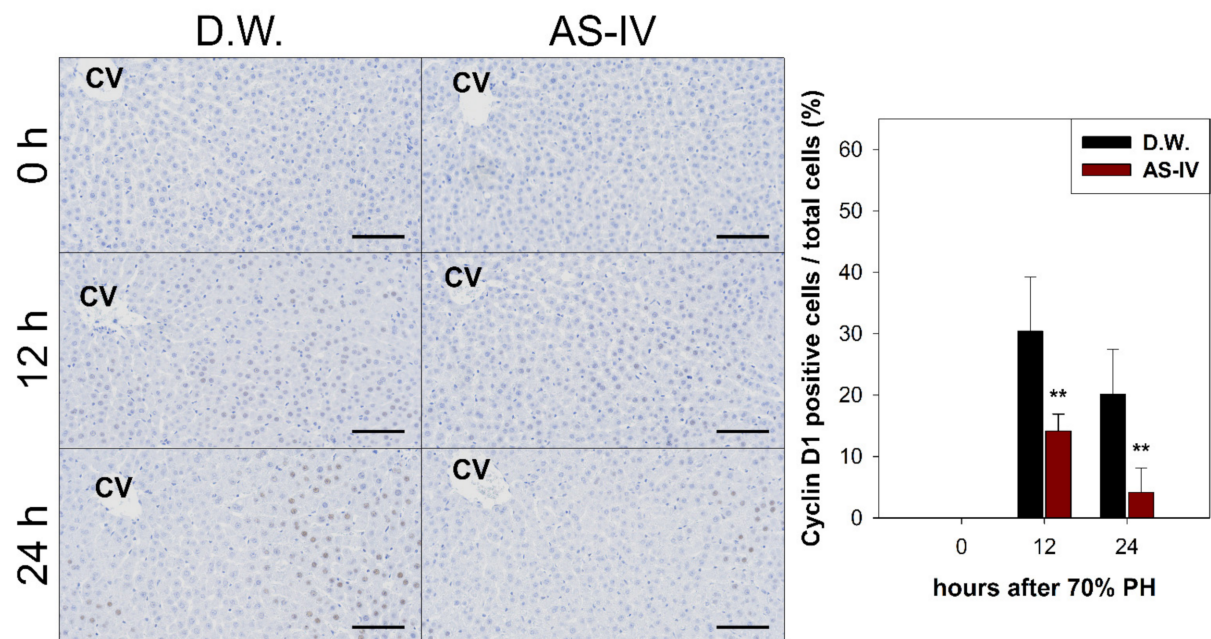


Figure 5. Immunostaining for cyclin D1. Cyclin D1 expression in regenerating liver tissues rapidly increased 12 h after PHx, peaking at 12 h after PHx then decreasing by 24 h. The AS-IV group showed a low expression of cyclin D1. Hematoxylin was used as a counter stain. (Scale bar indicates 100 μ m, CV: central vein, $n = 3$, mean \pm standard deviation, **: $p < 0.01$).

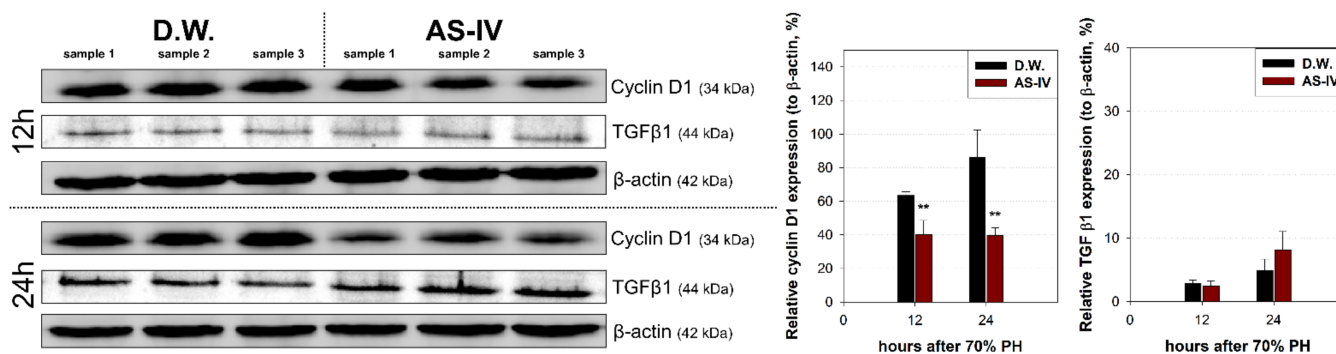


Figure 6. Relative expressions of cyclin D1 and TGF β 1. Expression of cyclin D1 and TGF β 1 were analyzed by Western blot analysis. 12 h after PHx, cyclin D1 expression decreased in the experimental group and decreased further by 24 h while showing increased TGF β 1 expression. Relative protein expressions are presented as a ratio of the β -actin loading control. (mean \pm standard deviation, $n = 3$, **: $p < 0.01$).

3. Discussion

Astragalus membranaceus is one of the oldest known medicinal plants in traditional Chinese medicine. The dried root of this plant is called huang qi and an astragaloside IV (AS-IV) is the core bio-active ingredient of huang qi. Recently, it was reported that AS-IV showed anti-oxidative, anti-cancer, and hepato-protective activity in a variety of experiments [41–43]. Looking at recent research, it seems likely that AS-IV has many pharmacological potential. In 2019 Wei et al. reported that AS-IV could improve liver cirrhosis [44]. However, the effects of AS-IV on liver regeneration have not yet been elucidated. The 70% partial hepatectomy (PHx) model has been used in numerous studies of liver regeneration. In this study, we investigated the effects of AS-IV on liver regeneration in a 70% PHx model using mRNA sequencing, immunohistochemistry, and Western blot analysis. Our results suggest that AS-IV could suppress liver regeneration after 70% PHx. After oral administration of AS-IV, many genes changed their expression significantly (Figure 2). To determine the effects of AS-IV, we focused on the functions that are carried out by a group of differently expressed genes (DEGs) rather than the increases or decreases in expression of each individual gene. From the fold change, corresponding protein interactions, and function annotation of DEGs, we found 20 key DEGs including *Mcm5*, *Cdc45*, *Cdc7*, *Cenpm*, *Asf1b*, *Donson*, *Tfdp2*, *Ccdc64*, *Cenpn*, *Brca2*, *Dbf4*, *Enahm*, *Mcm10*, *Ttk*, *Spd11*, *Cdc6*, *Ndc80*, *Kif20b*, *Rad9b*, and *Bora*, as shown in Figure 2e and Table 1. These genes showed strong functional relationship with cell division and our research suggests that these are the core genes responsible for the function of AS-IV in the regenerating liver. These results provide a potential mechanism for the therapeutic effects of AS-IV. Thus, as it relates to gene expression levels, by suppressing the genes required for molecular binding during DNA replication in the nucleus, AS-IV could inhibit DNA replication during cell division. These results suggest that AS-IV has a potent anti-proliferative effect in the regenerating liver.

DEGs were further analyzed via the KEGG pathway database to investigate the effects of AS-IV on proliferative signaling. Three signaling pathways (MAPK signaling pathway, PI3K-Akt signaling pathway, and cell cycle pathway) were down-regulated by AS-IV (Table 2, Figure 3). Other researchers have also reported similar down-regulation of MAPK signaling by AS-IV [45–47]. Decreased hepatocyte growth factor (HGF, hepato-proliferative signal molecule) and cyclin D1 (proliferation marker protein) expression also suggest the same anti-proliferative effects (Figures 4 and 5). Furthermore, AS-IV could affect the growth termination signal as well as could affect proliferative signal. Our extended study results show increased level of transforming growth factor β 1 (TGF β 1, growth termination signal) in the liver 24 h after PHx (Figure 6). In summary, AS-IV was revealed to have

anti-proliferative effects in the regenerating liver via changes in gene expressions and protein expressions related to cell division and proliferative signals.

And So, AS-IV showed anti-proliferative effects in regenerating liver tissues. Thus, for the purpose of tissue regeneration through encouraging normal cell division, it is likely that AS-IV is unsuitable for liver regeneration. However, AS-IV could be applied for other purposes, such as for reducing oxidative injury after PHx surgery. After PHx, the liver is rapidly regenerated. In parallel, oxidative stress also rapidly increased. Some reports have shown that AS-IV has anti-oxidative and hepato-protective activities [48,49]. Additionally, our results could be used as basic study data for the anti-cancer activities of AS-IV with other studies. In recent, similar anti-cancer effects of AS-IV were reported including blocking of MAPK signal, decreased PCNA and Ki67 expression, and triggering G1 arrest in tumor cell [45,50].

4. Materials and Methods

4.1. Animals and Experimental Design

Male rats (SD strain, 8 weeks) were obtained from DBL Co., Ltd. (Eumseong, Korea). They were housed in an environmentally controlled room at 25 ± 1 °C, 12/12-light/dark cycle, and relative humidity 60 ± 5 % with free access to standard food pellets and water (ad libitum). All animal experiments and procedures were performed in accordance with the guidelines for the care and use of laboratory animals of the national institutes of health (NIH) and after approval by the institutional animal care and use committee (IACUC) at the Soonchunhyang University (permission No.: SCH20-0002).

Rats were randomly divided into control and experimental groups depending on treatment and sacrifice time. Both groups consisted of six rats. Three rats of each group were sacrificed 12 h after PHx and the other three rats were sacrificed 24 h after PHx. The rats in the experimental group received intragastric administration of astragaloside IV (AS-IV, 10 mg/kg) [4,13,19,22,51]. AS-IV was diluted in 1.5 mL of D.W. [52]. AS-IV (product No. #A3305, purity > 98.0%, HPLC) was purchased from the Tokyo Chemical Industry Co., Ltd. (Tokyo, Japan). The rats in the control group received the same volume of D.W. by intragastric administration. AS-IV and D.W. were administrated 2 h before surgery (Figure 7) [53–58].

To establish the liver regeneration model, a 70% partial hepatectomy (PHx) involving resection of the median and left lateral lobes was performed under anesthesia as previously described by Higgins and Anderson [29]. Animals were fasted for 12 h before surgery. Rats were sacrificed at 12 or 24 h after 70% PHx [39]. Regenerated remnant liver tissue was collected for analyses.

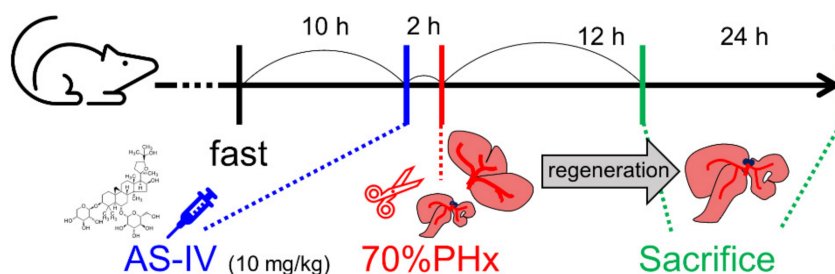


Figure 7. Administration of AS-IV and 70% PHx. Rats were received 10mg/kg of AS-IV diluted in D.W. (experimental group) or D.W. (control group) 2 h before 70% PHx and were sacrificed at 12 h or 24 h after PHx.

4.2. RNA Sequencing Analysis

TRIzol[®] reagent (Invitrogen, Carlsbad, CA, USA) was used for isolation of total RNA from liver tissue [59]. cDNA libraries were generated and purified using QuantSeq 3' mRNA-Seq Library Prep Kit for Illumina (LEXOGEN, Vienna, Austria) according to manu-

facturer's instructions. High-throughput sequencing was performed as single-end 75 base pair sequencing using a NextSeq 500 (Illumina, Inc., San Diego, CA, USA). Raw reads were processed by BBDuk and aligned to the reference genome (rat, rn6, UCSC) using Bowtie2 [60]. The alignment file was assembled and estimated their abundances. Differentially expressed genes (DEGs) were determined based on counts from unique and multiple alignments with coverage in the Bedtools. The read count data were processed based on a quantile normalization method using EdgeR within R [61]. Genes were classified based on the database for annotation, visualization and integrated discovery (DAVID) and Medline databases (<http://david.abcc.ncifcrf.gov/>, accessed on 8 November 2020). DEGs exhibiting changes more than 2-fold were considered significant [59]. DEGs were also analyzed via the Kyoto Encyclopedia of Genes and Genomes (KEGG) mapper (address: https://www.genome.jp/kegg/tool/map_pathway2.html, accessed on 8 November 2020). DEGs were also analyzed based on protein-protein interactions via multiple protein searching tool within STRING database (ver. 11.0, address: <http://string-db.org/db.org/>, accessed on 8 November 2020).

4.3. Immunohistochemistry

Liver tissue was removed and immediately fixed in 10% neutral buffered formalin. It was then embedded in paraffin according to the routine process for light microscopy. The paraffin block was then cut into 4 μm thicknesses by rotary microtome (RM2235, Leica Biosystems, Germany). Antigen retrieval was conducted with sodium citrate buffer (10 mM, pH 6.0) at 95 °C. Heated sections were cooled for 30 min at room temperature. Sections were then incubated in 3% H_2O_2 (#1146, DUCSAN PURE CHEMICALS, Korea) and incubated in 5% bovine serum albumin (BSA, A7906, Merck KGaA, Darmstadt, Germany). Primary antibodies against Cyclin D1 (ab134175, Abcam plc., UK) and HGF (ab83760, Abcam plc., UK) were added. An HRP-conjugated secondary antibody (Thermo fisher scientific, Waltham, MA, USA) was then added. Immuno-detection was conducted with 3,3'-diaminobenzidine (SIGMAFAST™, Merck KGaA, Darmstadt, Germany). Counter staining was conducted using hematoxylin. All procedures were carried out in a humidified chamber to prevent the drying out of tissues. Tissues were observed using a microscope (CKX53, Olympus, Tokyo, Japan). Counts of positive reacted cells and total cells were measured by the color deconvolution tool within TMAPKER (Ver. 2.146, open-source software) [62,63].

4.4. Western Blot Analysis

Total protein was extracted from liver tissues using protein extraction solution (PRO-PREP™, iNtRON BIOTECHNOLOGY, Seongnam, Korea) on ice and was determined by bicinchoninate (BCA) calorimetric assay kit (#23227, Thermo fisher scientific, USA) according to manufacturer's instruction. The protein was separated by 12% SDS-PAGE and transferred to PVDF (IPVH00010, Merck KGaA, Germany). The PVDF was then blocked with 5% skim milk (#232100, BD, Franklin Lakes, NJ, USA) and incubated with a primary antibody diluted in 0.5% skim milk overnight at 4 °C. The primary antibody against β -actin (A5316, Merck KGaA, Darmstadt, Germany) was diluted to 1:6000. Primary antibodies against cyclin D1 (ab134175) and TGF β 1 (ab92486) were purchased from Abcam plc. (Cambridge, UK) and diluted to 1:3000. The membrane was further incubated with an HRP-conjugated secondary antibody (Thermo fisher scientific, USA) at room temperature for 1 h, followed by washing with PBS. Protein expression was detected by enhanced chemiluminescence (ECL) solution (K-12049-D50, Advansta Inc., San Jose, CA, USA) and chemiluminescence imaging system (GBox ichemi XL, Syngene, UK). β -actin was used as loading control. The relative expression level of target protein was expressed as ratio of β -actin [64].

4.5. Statistical Analysis

All quantitative data are presented as mean \pm standard deviation (SD) from three independent experiments. Statistical analyses were performed using IBM SPSS statistics for windows (ver. 25, IBM, New York, NY, USA). Student's *t*-tests were used to analyze differences between control and the experimental group. Data with a *p*-value less than 0.05 were considered statistically significant. (*: *p*-value < 0.05, **: *p*-value < 0.01)

5. Conclusions

Astragaloside IV (AS-IV) is the major bio-active component of Huang Qi (the dried root of *Astragalus membranaceus*, a traditional Chinese medicinal plant). In present study, we demonstrated the pharmacological effects of AS-IV on regenerating rat liver tissue after 70% partial hepatectomy. AS-IV down-regulated proliferative signals, genes related to DNA replication, and cyclin D1 expression (Figure 8). In conclusion, AS-IV showed anti-proliferative activities in regenerating liver tissue.

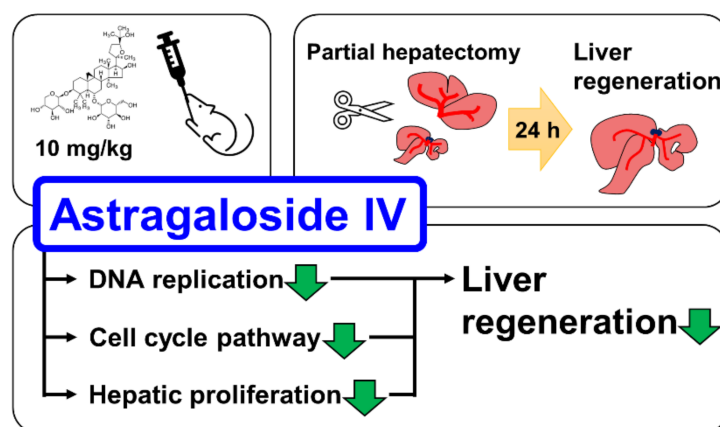


Figure 8. Graphical abstract of study. AS-IV suppressed hepatic proliferation of regenerating liver tissues after 70% PHx.

Author Contributions: Conceptualization: G.-S.L. and W.-J.K.; methodology: G.-S.L. and E.-G.J.; software: G.-S.L. and Y.-S.L.; validation: G.-S.L. and K.-W.N.; formal analysis: G.-S.L.; investigation: G.-S.L., H.-Y.J., H.-G.Y. and Y.-R.S.; resources: H.-Y.J., H.-G.Y. and Y.-R.S.; data curation: H.-Y.J. and H.-G.Y.; writing—original draft preparation: G.-S.L.; writing—review and editing: E.-G.J., Y.-S.L., K.-W.N. and W.-J.K.; visualization: G.-S.L., H.-Y.J. and H.-G.Y.; supervision: W.-J.K.; project administration: G.-S.L.; funding acquisition: E.-G.J., Y.-S.L., K.-W.N. and W.-J.K. All authors have read and agreed to the published version of the manuscript.

Funding: This work was supported by the Soonchunhyang University Research Fund.

Institutional Review Board Statement: The study was conducted according to the guidelines for the care and use of laboratory animal of the national institutes of health (NIH) and approved by the institutional animal care and use committee (IACUC) at the Soonchunhyang University (protocol No.: SCH20-0002, approved at February 2020).

Informed Consent Statement: Not applicable.

Data Availability Statement: We want to exclude this statement. Our study did not report public dataset.

Acknowledgments: This work was supported by the Soonchunhyang University Research Fund.

Conflicts of Interest: The authors declare no conflict of interest.

Sample Availability: Astragaloside IV is available from the authors or Tokyo Chemical Industry Co., Ltd. (Tokyo, Japan). Product No. #3305.

References

1. Fu, J.; Wang, Z.; Huang, L.; Zheng, S.; Wang, D.; Chen, S.; Zhang, H.; Yang, S. Review of the Botanical Characteristics, Phytochemistry, and Pharmacology of *Astragalus Membranaceus* (Huangqi). *Phytother. Res.* **2014**, *28*, 1275–1283. [[CrossRef](#)] [[PubMed](#)]
2. Liu, P.; Zhao, H.; Luo, Y. Anti-aging Implications of *Astragalus Membranaceus* (Huangqi): A Well-known Chinese Tonic. *Aging Dis.* **2017**, *8*, 868–886. [[CrossRef](#)] [[PubMed](#)]
3. Ma, X.Q.; Shi, Q.; Duan, J.A.; Dong, T.T.; Tsim, K.W. Chemical Analysis of *Radix Astragali* (Huangqi) in China: A Comparison with Its Adulterants and Seasonal Variations. *J. Agric. Food Chem.* **2002**, *50*, 4861–4866. [[CrossRef](#)] [[PubMed](#)]
4. Guo, Z.; Lou, Y.; Kong, M.; Luo, Q.; Liu, Z.; Wu, J. A Systematic Review of Phytochemistry, Pharmacology and Pharmacokinetics on *Astragali Radix*: Implications for *Astragali Radix* as a Personalized Medicine. *Int. J. Mol. Sci.* **2019**, *20*, 1463. [[CrossRef](#)]
5. Hao, X.; Wang, P.; Ren, Y.; Liu, G.; Zhang, J.; Leury, B.; Zhang, C. Effects of *Astragalus Membranaceus* Roots Supplementation on Growth Performance, Serum Antioxidant and Immune Response in Finishing Lambs. *Asian Australas J. Anim. Sci.* **2020**, *33*, 965–972. [[CrossRef](#)]
6. Ren, S.; Zhang, H.; Mu, Y.; Sun, M.; Liu, P. Pharmacological Effects of Astragaloside IV: A Literature Review. *J. Tradit. Chin. Med.* **2013**, *33*, 413–416. [[CrossRef](#)]
7. Zhao, M.; Gödecke, T.; Gunn, J.; Duan, J.A.; Che, C.T. Protostane and Fusidane Triterpenes: A Mini-Review. *Molecules* **2013**, *18*, 4054–4080. [[CrossRef](#)]
8. Živný, P.; Živná, H.; Palička, V.; Žaloudková, L.; Mocková, P.; Cermanová, J.; Mičuda, S. Modulation of Rat Liver Regeneration after Partial Hepatectomy by Dietary Cholesterol. *Acta Med.* **2018**, *61*, 22–28. [[CrossRef](#)]
9. Tsugawa, Y.; Natori, M.; Handa, H.; Imai, T. Estradiol Accelerates Liver Regeneration through Estrogen Receptor α . *Clin. Exp. Gastroenterol.* **2019**, *12*, 331–336. [[CrossRef](#)]
10. Li, X.; Wang, X.; Han, C.; Wang, X.; Xing, G.; Zhou, L.; Li, G.; Niu, Y. Astragaloside IV Suppresses Collagen Production of Activated Hepatic Stellate Cells via Oxidative Stress-mediated p38 MAPK Pathway. *Free Radic. Biol. Med.* **2013**, *60*, 168–176. [[CrossRef](#)]
11. Yu, W.; Lv, Z.; Zhang, L.; Gao, Z.; Chen, X.; Yang, X.; Zhong, M. Astragaloside IV Reduces the Hypoxia-Induced Injury in PC-12 Cells by Inhibiting Expression of miR-124. *Biomed. Pharmacother.* **2018**, *106*, 419–425. [[CrossRef](#)]
12. Gong, L.; Chang, H.; Zhang, J.; Guo, G.; Shi, J.; Xu, H. Astragaloside IV Protects Rat Cardiomyocytes from Hypoxia-Induced Injury by Down-Regulation of miR-23a and miR-92a. *Cell Physiol. Biochem.* **2018**, *49*, 2240–2253. [[CrossRef](#)]
13. Jiang, M.; Ni, J.; Cao, Y.; Xing, X.; Wu, Q.; Fan, G. Astragaloside IV Attenuates Myocardial Ischemia-Reperfusion Injury from Oxidative Stress by Regulating Succinate, Lysophospholipid Metabolism, and ROS Scavenging System. *Oxidative Med. Cell. Longev.* **2019**, *2019*, 9137654. [[CrossRef](#)]
14. Wei, D.; Xu, H.; Gai, X.; Jiang, Y. Astragaloside IV Alleviates Myocardial Ischemia-Reperfusion Injury in Rats through Regulating PI3K/AKT/GSK-3 β Signaling Pathways. *Acta Cir. Bras.* **2019**, *34*, e201900708. [[CrossRef](#)]
15. He, Y.; Xi, J.; Zheng, H.; Zhang, Y.; Jin, Y.; Xu, Z. Astragaloside IV Inhibits Oxidative Stress-Induced Mitochondrial Permeability Transition Pore Opening by Inactivating GSK-3 β via Nitric Oxide in H9c2 Cardiac Cells. *Oxidative Med. Cell Longev.* **2012**, *2012*, 935738. [[CrossRef](#)]
16. Jiang, K.; Lu, Q.; Li, Q.; Ji, Y.; Chen, W.; Xue, X. Astragaloside IV Inhibits Breast Cancer Cell Invasion by Suppressing Vav3 Mediated Rac1/MAPK Signaling. *Int. Immunopharmacol.* **2017**, *42*, 195–202. [[CrossRef](#)]
17. Cheng, X.; Gu, J.; Zhang, M.; Yuan, J.; Zhao, B.; Jiang, J.; Jia, X. Astragaloside IV Inhibits Migration and Invasion in Human Lung Cancer A549 Cells via Regulating PKC- α -ERK1/2-NF- κ B Pathway. *Int. Immunopharmacol.* **2014**, *23*, 304–313. [[CrossRef](#)]
18. Wang, N.; Siu, F.; Zhang, Y. Effect of Astragaloside IV on Diabetic Gastric Mucosa in Vivo and in Vitro. *Am. J. Transl. Res.* **2017**, *9*, 4902–4913.
19. Fan, Y.; Fan, H.; Zhu, B.; Zhou, Y.; Liu, Q.; Li, P. Astragaloside IV Protects Against Diabetic Nephropathy via Activating eNOS in Streptozotocin Diabetes-Induced Rats. *BMC complementary Altern. Med.* **2019**, *19*, 355. [[CrossRef](#)]
20. Ding, Y.; Yuan, S.; Liu, X.; Mao, P.; Zhao, C.; Huang, Q.; Zhang, R.; Fang, Y.; Song, Q.; Yuan, D.; et al. Protective Effects of Astragaloside IV on db/db Mice with Diabetic Retinopathy. *PLoS ONE* **2014**, *9*, e112207. [[CrossRef](#)]
21. Luo, X.; Huang, P.; Yuan, B.; Liu, T.; Lan, F.; Lu, X.; Dai, L.; Liu, Y.; Yin, H. Astragaloside IV Enhances Diabetic Wound Healing Involving Upregulation of Alternatively Activated Macrophages. *Int. Immunopharmacol.* **2016**, *35*, 22–28. [[CrossRef](#)]
22. Zhao, X.M.; Zhang, J.; Liang, Y.N.; Niu, Y.C. Astragaloside IV Synergizes with Ferulic Acid to Alleviate Hepatic Fibrosis in Bile Duct-ligated Cirrhotic Rats. *Dig. Dis. Sci.* **2020**, *65*, 2925–2936. [[CrossRef](#)]
23. Liu, H.; Wei, W.; Sun, W.Y.; Li, X. Protective Effects of Astragaloside IV on Porcine-Serum-Induced Hepatic Fibrosis in Rats and in Vitro Effects on Hepatic Stellate Cells. *J. Ethnopharmacol.* **2009**, *122*, 502–508. [[CrossRef](#)]
24. Xie, D.; Zhou, P.; Liu, L.; Jiang, W.; Xie, H.; Zhang, L.; Xie, D. Protective Effect of Astragaloside IV on Hepatic Injury Induced by Iron Overload. *Biomed. Res. Int.* **2019**, *2019*, 3103946. [[CrossRef](#)]
25. Wang, S.; Li, J.; Huang, H.; Gao, W.; Zhuang, C.; Li, B.; Zhou, P.; Kong, D. Anti-hepatitis B Virus Activities of Astragaloside IV Isolated from *Radix Astragali*. *Biol. Pharm. Bull.* **2009**, *32*, 132–135. [[CrossRef](#)]
26. Yagi, S.; Hirata, M.; Miyachi, Y.; Uemoto, S. Liver Regeneration after Hepatectomy and Partial Liver Transplantation. *Int. J. Mol. Sci.* **2020**, *21*, 8414. [[CrossRef](#)]
27. Michalopoulos, G.K.; de Frances, M.C. Liver Regeneration. *Science* **1997**, *276*, 60–66. [[CrossRef](#)]

28. Andersen, K.J.; Knudsen, A.R.; Kannerup, A.S.; Sasanuma, H.; Nyengaard, J.R.; Hamilton-Dutoit, S.; Erlandsen, E.J.; Jørgensen, B.; Mortensen, F.V. The Natural History of Liver Regeneration in Rats: Description of an Animal Model for Liver Regeneration Studies. *Int. J. Surg.* **2013**, *11*, 903–908. [[CrossRef](#)]
29. Higgins, G.M.; Anderson, R.M. Experimental Pathology of Liver: Restoration of the Liver of the White Rat Following Partial Surgical Removal. *Arch. Pathol.* **1931**, *12*, 186–202.
30. Madrahimov, N.; Dirsch, O.; Broelsch, C.; Dahmen, U. Marginal Hepatectomy in the Rat: From Anatomy to Surgery. *Ann. Surg.* **2006**, *244*, 89–98. [[CrossRef](#)]
31. Huisman, F.; van Lienden, K.P.; Damude, S.; Hoekstra, L.T.; van Gulik, T.M. A Review of Animal Models for Portal Vein Embolization. *J. Surg. Res.* **2014**, *191*, 179–188. [[CrossRef](#)] [[PubMed](#)]
32. Taub, R. Liver Regeneration: From Myth to Mechanism. *Nat. Rev. Mol. Cell Biol.* **2004**, *5*, 836–847. [[CrossRef](#)] [[PubMed](#)]
33. Kwon, Y.J.; Lee, K.G.; Choi, D. Clinical Implications of Advances in Liver Regeneration. *Clin. Mol. Hepatol.* **2015**, *21*, 7–13. [[CrossRef](#)] [[PubMed](#)]
34. Cienfuegos, J.A.; Rotellar, F.; Baixauli, J.; Martínez-Regueira, F.; Pardo, F.; Hernández-Lizoáin, J.L. Liver Regeneration—The Best Kept Secret. A Model of Tissue Injury Response. *Rev. Esp. Enferm. Dig.* **2014**, *106*, 171–194.
35. Kang, L.I.; Mars, W.M.; Michalopoulos, G.K. Signals and Cells Involved in Regulating Liver Regeneration. *Cells* **2012**, *1*, 1261–1292. [[CrossRef](#)] [[PubMed](#)]
36. Hoffmann, K.; Nagel, A.J.; Tanabe, K.; Fuchs, J.; Dehlke, K.; Ghamarnejad, O.; Lemekhova, A.; Mehrabi, A. Markers of Liver Regeneration—the Role of Growth Factors and Cytokines: A Systematic Review. *BMC Surg.* **2020**, *20*, 31. [[CrossRef](#)] [[PubMed](#)]
37. Tarlá, M.R.; Ramalho, F.; Ramalho, L.N.; Silva Tde, C.; Brandão, D.F.; Ferreira, J.; Silva Ode, C.; Zucoloto, S. Cellular Aspects of Liver Regeneration. *Acta Cir. Bras.* **2006**, *21*, 63–66. [[CrossRef](#)]
38. Ozaki, M. Cellular and Molecular Mechanisms of Liver Regeneration: Proliferation, Growth, Death and Protection of Hepatocytes. *Semin. Cell Dev. Biol.* **2020**, *100*, 62–73. [[CrossRef](#)]
39. Rychtrmoc, D.; Libra, A.; Buncek, M.; Garnol, T.; Cervinková, Z. Studying Liver Regeneration by Means of Molecular Biology: How Far We are in Interpreting the Findings? *Acta Med.* **2009**, *52*, 91–99. [[CrossRef](#)]
40. Abu Rmilah, A.; Zhou, W.; Nelson, E.; Lin, L.; Amiot, B.; Nyberg, S.L. Understanding the Marvels Behind Liver Regeneration. *Wiley Interdiscip. Rev. Dev. Biol.* **2019**, *8*, e340. [[CrossRef](#)]
41. Yang, S.; Zhang, R.; Xing, B.; Zhou, L.; Zhang, P.; Song, L. Astragaloside IV Ameliorates Preeclampsia-Induced Oxidative Stress through the Nrf2/HO-1 Pathway in a Rat Model. *Am. J. Physiol. Endocrinol. Metab.* **2020**, *319*, E904–E911. [[CrossRef](#)]
42. Cui, X.; Jiang, X.; Wei, C.; Xing, Y.; Tong, G. Astragaloside IV Suppresses Development of Hepatocellular Carcinoma by Regulating miR-150-5p/ β -catenin Axis. *Environ. Toxicol. Pharmacol.* **2020**, *78*, 103397. [[CrossRef](#)]
43. Han, L.; Li, J.; Lin, X.; Ma, Y.F.; Huang, Y.F. Protective Effect of Astragaloside IV on Oxidative Damages of Change Liver Cell Induced by Ethanol and H₂O₂. *Zhongguo Zhongyao Zazhi* **2014**, *39*, 4430–4435.
44. Wei, R.; Liu, H.; Chen, R.; Sheng, Y.; Liu, T. Astragaloside IV Combating Liver Cirrhosis through the PI3K/Akt/mTOR Signaling Pathway. *Exp. Ther. Med.* **2019**, *17*, 393–397. [[CrossRef](#)]
45. Li, B.; Wang, F.; Liu, N.; Shen, W.; Huang, T. Astragaloside IV Inhibits Progression of Glioma via Blocking MAPK/ERK Signaling Pathway. *Biochem. Biophys. Res. Commun.* **2017**, *491*, 98–103. [[CrossRef](#)]
46. Leng, B.; Li, C.; Sun, Y.; Zhao, K.; Zhang, L.; Lu, M.L.; Wang, H.X. Protective Effect of Astragaloside IV on High Glucose-Induced Endothelial Dysfunction via Inhibition of P2X7R Dependent P38 MAPK Signaling Pathway. *Oxidative Med. Cell Longev.* **2020**, *2020*, 5070415. [[CrossRef](#)]
47. Hsieh, H.L.; Liu, S.H.; Chen, Y.L.; Huang, C.Y.; Wu, S.J. Astragaloside IV Suppresses Inflammatory Response via Suppression of NF- κ B, and MAPK Signaling in Human Bronchial Epithelial Cells. *Arch. Physiol. Biochem.* **2020**, *14*, 1–10. [[CrossRef](#)]
48. Zhu, Z.; Li, J.; Zhang, X. Astragaloside IV Protects Against Oxidized Low-Density Lipoprotein (ox-LDL)-Induced Endothelial Cell Injury by Reducing Oxidative Stress and Inflammation. *Med. Sci. Monit.* **2019**, *25*, 2132–2140. [[CrossRef](#)]
49. Nie, Q.; Zhu, L.; Zhang, L.; Leng, B.; Wang, H. Astragaloside IV Protects Against Hyperglycemia-Induced Vascular Endothelial Dysfunction by Inhibiting Oxidative Stress and Calpain-1 Activation. *Life Sci.* **2019**, *232*, 116662. [[CrossRef](#)]
50. Su, C.M.; Wang, H.C.; Hsu, F.T.; Lu, C.H.; Lai, C.K.; Chung, J.G.; Kuo, Y.C. Astragaloside IV Induces Apoptosis, G1-Phase Arrest and Inhibits Anti-apoptotic Signaling in Hepatocellular Carcinoma. *In Vivo* **2020**, *34*, 631–638. [[CrossRef](#)]
51. Lv, L.; Wu, S.Y.; Wang, G.F.; Zhang, J.J.; Pang, J.X.; Liu, Z.Q.; Xu, W.; Wu, S.G.; Rao, J.J. Effect of Astragaloside IV on Hepatic Glucose-Regulating Enzymes in Diabetic Mice Induced by a High-Fat Diet and Streptozotocin. *Phytother. Res.* **2010**, *24*, 219–224. [[CrossRef](#)]
52. Gad, S.C.; Cassidy, C.D.; Aubert, N.; Spainhour, B.; Robbe, H. Nonclinical Vehicle Use in Studies by Multiple Routes in Multiple Species. *Int. J. Toxicol.* **2006**, *25*, 499–521. [[CrossRef](#)]
53. Gu, Y.; Wang, G.; Fawcett, J.P. Determination of Astragaloside IV in Rat Plasma by Liquid Chromatography Electrospray Ionization Mass Spectrometry. *J. Chromatogr. B Analyt. Technol. Biomed. Life Sci.* **2004**, *801*, 285–288. [[CrossRef](#)]
54. Shi, X.; Tang, Y.; Zhu, H.; Li, W.; Li, Z.; Li, W.; Duan, J.A. Comparative Tissue Distribution Profiles of Five Major Bio-active Components in Normal and Blood Deficiency Rats after Oral Administration of Danggui Buxue Decoction by UPLC-TQ/MS. *J. Pharm. Biomed. Anal.* **2014**, *88*, 207–215. [[CrossRef](#)]

55. Liu, X.H.; Zhao, J.B.; Guo, L.; Yang, Y.L.; Hu, F.; Zhu, R.J.; Feng, S.L. Simultaneous Determination of Calycosin-7-O- β -D-Glucoside, Ononin, Calycosin, Formononetin, Astragaloside IV, and Astragaloside II in Rat Plasma after Oral Administration of Radix Astragali Extraction for Their Pharmacokinetic Studies by Ultra-pressure Liquid Chromatography with Tandem Mass Spectrometry. *Cell Biochem. Biophys.* **2014**, *70*, 677–686. [[CrossRef](#)]
56. Zhang, H.; Song, J.; Dai, H.; Liu, Y.; Wang, L. Effects of Puerarin on the Pharmacokinetics of Astragaloside IV in Rats and Its Potential Mechanism. *Pharm. Biol.* **2020**, *58*, 328–332. [[CrossRef](#)]
57. Chang, Y.X.; Sun, Y.G.; Li, J.; Zhang, Q.H.; Guo, X.R.; Zhang, B.L.; Jin, H.; Gao, X.M. The Experimental Study of *Astragalus Membranaceus* on Meridian Tropism: The Distribution Study of Astragaloside IV in Rat Tissues. *J. Chromatogr. B Analyt. Technol. Biomed. Life Sci.* **2012**, *911*, 71–75. [[CrossRef](#)]
58. Zhang, W.D.; Zhang, C.; Liu, R.H.; Li, H.L.; Zhang, J.T.; Mao, C.; Moran, S.; Chen, C.L. Preclinical Pharmacokinetics and Tissue Distribution of a Natural Cardioprotective Agent Astragaloside IV in Rats and Dogs. *Life Sci.* **2006**, *79*, 808–815. [[CrossRef](#)]
59. Colak, D.; Al-Harazi, O.; Mustafa, O.M.; Meng, F.; Assiri, A.M.; Dhar, D.K.; Broering, D.C. RNA-Seq Transcriptome Profiling in Three Liver Regeneration Models in Rats: Comparative Analysis of Partial Hepatectomy, ALLPS, and PVL. *Sci. Rep.* **2020**, *10*, 5213. [[CrossRef](#)] [[PubMed](#)]
60. Langmead, B.; Salzberg, S.L. Fast Gapped-read Alignment with Bowtie 2. *Nat. Methods* **2012**, *9*, 357–359. [[CrossRef](#)]
61. Robinson, M.D.; McCarthy, D.J.; Smyth, G.K. EdgeR: A Bioconductor Package for Differential Expression Analysis of Digital Gene Expression Data. *Bioinformatics* **2010**, *26*, 139–140. [[CrossRef](#)] [[PubMed](#)]
62. Schüffler, P.J.; Fuchs, T.J.; Ong, C.S.; Wild, P.J.; Rupp, N.J.; Buhmann, J.M. TMARKER: A Free Software Toolkit for Histopathological Cell Counting and Staining Estimation. *J. Pathol. Inform.* **2013**, *4*, S2. [[CrossRef](#)] [[PubMed](#)]
63. Zhong, Q.; Rüschoff, J.H.; Guo, T.; Gabrani, M.; Schüffler, P.J.; Rechsteiner, M.; Liu, Y.; Fuchs, T.J.; Rupp, N.J.; Fankhauser, C.; et al. Image-based Computational Quantification and Visualization of Genetic Alterations and Tumour Heterogeneity. *Sci. Rep.* **2016**, *6*, 24146. [[CrossRef](#)] [[PubMed](#)]
64. Lee, G.S.; Yang, H.G.; Kim, J.H.; Ahn, Y.M.; Han, M.D.; Kim, W.J. Pine (*Pinus Densiflora*) Needle Extract Could Promote the Expression of PCNA and Ki-67 after Partial Hepatectomy in Rat. *Acta Cir. Bras.* **2019**, *34*, e201900606. [[CrossRef](#)]